

A Solar Photovoltaic Performance Monitoring and Statistical Forecasting Model Using a Multi-Layer Feed-Forward Neural Network and Artificial Intelligence

G. Kumaravel*¹  , S. Kirthiga²  , Mohammed Mahmood Hamed Al Shekaili¹  , Qais Hamed Saif Abdullah AL Othmani¹  

¹Engineering Department, University of Technology and Applied Sciences, Ibri, Oman.

²Electrical division, Unique design steel and welding LLC, Dubai, United Arab Emirates.

*Corresponding Author.

ICCDA2023: International Conference on Computing and Data Analytics 2023.

Received 18/01/2024, Revised 19/04/2024, Accepted 21/04/2024, Published 25/05/2024



© 2022 The Author(s). Published by College of Science for Women, University of Baghdad.

This is an open-access article distributed under the terms of the [Creative Commons Attribution 4.0 International License](https://creativecommons.org/licenses/by/4.0/), which permits unrestricted use, distribution, and reproduction in any medium, provided the original work is properly cited.

Abstract

The topographical nature of the Sultanate of Oman makes the solar power system a viable and reliable option for bulk power production in the renewable energy market. Many desert areas of Oman experience high levels of solar radiation. This is suitable for photovoltaic (PV) systems as their efficiency mainly depends on solar radiation. However, in real-time applications, many environmental factors affect the efficiency of the solar panel and therefore its performance. In this article, the Multilayer Feed Forward Neural Network (MFFN) is proposed to track the solar PV system performance in order to replace or improve the performance of the solar PV system based on its current state. A backpropagation algorithm (BPA) is used to train the MFFN.

Keywords: Back propagation algorithm, Multi-layer Feed Forward network, Photovoltaic system, Renewable energy, Solar power system.

Introduction

PV panels are used to convert solar energy into electrical energy using semiconductor technology. It produces electricity based on the solar radiation at the location. Recently, PV power systems are gaining momentum. It is considered clean energy because it has almost no carbon footprint. It is also considered maintenance-free and reliable compared to renewable energy systems¹⁻³.

However, the output of the solar PV system is usually variable as its output depends on the solar radiation in the solar panel. Currently, on grid and off grid solar PV systems are used for bulk power production

in the renewable energy industries. The voltage fluctuation in the standalone solar PV power system has significant effects on the load side^{4,5}. On the other hand, voltage fluctuations in grid-connected solar PV systems affect the stability of the grid voltage^{6,7}.

As grid-tied solar PV systems are becoming increasingly popular in Oman. It is necessary to analyze the advantages and disadvantages of this system in order to maintain voltage stability in the utility network. Since power fluctuations due to solar PV systems affect the stability of the grid system, a

suitable system is required to predict possible fluctuations in the system.

Due to climatic uncertainty. It is very difficult to predict solar PV system performance based on just one set of measurements. In order to predict the actual value of the parameters in the PV power system, repeated measurement and analysis are

required. Because the performance of the PV power system depends on solar radiation, which is influenced by many parameters such as temperature, humidity, sky cover and wind speed. Therefore, an appropriate monitoring and forecasting system is required to maintain the efficiency at an optimal level, which is very important for the stability of the network⁸⁻¹⁰.

Solar Photovoltaic Monitoring and Forecasting System

Solar PV module monitoring and forecasting system is a complex task involving various parameters. The parameters mainly depend on the site conditions and the parameters relevant to the PV modules. The monitoring and forecasting systems are roughly divided into physical and stochastic models.

In the physical model, electricity production from PV modules is predicted based on global solar radiation. It is based solely on mathematical formulas and equations. The topographical characteristics and climatic conditions at the location are not taken into account in this method^{11,12}. Therefore, this method only provides approximate results of the forecast of the respective PV power system. The actual output power of the PV system is predicted based on the solar radiation at ground level for an hour or minutes. This method provides very accurate results because the climatic conditions at the site are nonlinear¹³.

Many artificial intelligences (AI) and machine-learning based systems are used to predict the forecast of solar PV systems. Examples of this category include Artificial Neural Networks (ANN), Adaptive Neuro Fuzzy Inference System (ANFIS), genetic algorithms, Particle Swarm Optimization (PSO), and deep learning.

This article proposes an AI and ANN based solar PV monitoring and forecasting system, it is a static method. Therefore, the output power of the solar PV systems is predicted based on global solar irradiance based on the geographical location. The AI is used to estimate the output power of the solar PV system based on the annual global irradiance and the average temperature at the site. By considering this data as a

target, the ANN is used to monitor the solar PV system performance.

Multilayer Feed Forward Neural Network

In this article, the ANN is realized by implementing an MFFN network. The MFFN network is trained using the backpropagation algorithm¹⁴⁻¹⁶.

Architecture

The structure of the MFFN is shown in Fig. 1. The nodes of the input layer (x_1, x_2, \dots, x_n) are linked to the nodes of the hidden layer (h_1, h_2, \dots, h_m) with the weights V . Similarly, the hidden layer nodes are linked to the output layer nodes (y_1, y_2, \dots, y_n) with weights W .

The input of the first node of the hidden layer is calculated as follows

$$a_1 = V_{11}x_1 + \dots + V_{1n}x_n \quad 1$$

Similarly, the input of the m^{th} node is calculated as follows

$$a_m = V_{m1}x_1 + \dots + V_{mn}x_n \quad 2$$

then mathematically, the first node of the hidden layer is represented by the activation function as follows

$$h_1 = \frac{1}{1+e^{-a_1}} \quad 3$$

Similarly, the activation function of an m^{th} node of a hidden layer is represented as

$$h_m = \frac{1}{1+e^{-a_m}} \quad 4$$

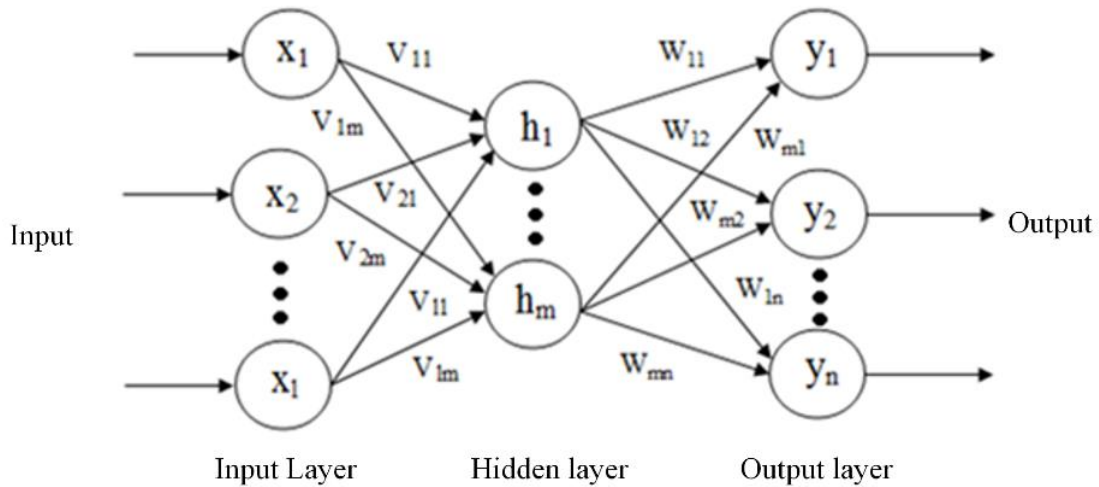


Figure 1. The architecture of MFFN network

The input of the first node of the output layer is calculated as follows

$$b_1 = W_{11}h_1 + \dots + W_{m1}h_m \quad 5$$

Similarly, the input of the n^{th} node is calculated as

$$b_n = W_{1n}h_1 + \dots + W_{mn}h_m \quad 6$$

Then mathematically, the first node of the output layer is represented by the activation function as

$$y_1 = \frac{1}{1+e^{-b_1}} \quad 7$$

Similarly, the activation function of an m^{th} node of a hidden layer is represented as

$$y_n = \frac{1}{1+e^{-b_n}} \quad 8$$

Back Propagation Algorithm

The MFFN is trained by BPA. the detailed procedure of BPA is given below.

The input data set is assumed as

$$\{X\}_{IL \ l*1} = \begin{bmatrix} V_t \\ P_t \end{bmatrix}_{2*1} \quad 9$$

Here, V_t and P_t represent the normalized value of the voltage and power produced by the solar PV system. The normalized output obtained from the MFFN network is represented by

$$\{Y\}_{OL \ n*1} = \begin{bmatrix} V_t \\ P_t \end{bmatrix}_{2*1} \quad 10$$

Here, V_t represents the output voltage and P_t represents the output current of the solar PV system for the average temperature at the site.

By linear activation function,

$$\{Y\}_{IL \ l*1} = \{X\}_{IL \ l*1} \quad 11$$

Here $\{Y\}_{IL}$ represents the output of the input layer and $\{X\}_{IL}$ represents the input of the input layer.

The hidden layer input is calculated by

$$\{X\}_{HL \ m*1} = [V]_{m*1}^T \{Y\}_{IL \ l*1} \quad 12$$

Here, V represents the weight of the input to hidden layer weights and $\{X\}_{HL}$ represents the input of the hidden layer. Then, the output of the hidden layer is calculated by

$$\{Y\}_{HL} = \left\{ \frac{1}{1+e^{-1_{HLi}}} \right\}_{m*1} \quad 13$$

Then the input of the output layer is estimated by

$$\{X\}_{OL \ n*1} = [W]_{n*m}^T \{Y\}_{HL \ m*1} \quad 14$$

Here, W represents the hidden-output layer weights. Then the output of the output layer is calculated by

$$\{Y\}_{OL} = \left\{ \frac{1}{(1+e^{-1_{OLj}})} \right\} \quad 15$$

$$\text{Error}_p = \sqrt{\frac{\sum(B_j - Y_{OLj})^2}{n}} \quad 16$$

The deviation $\{D\}$ is calculated by

$$\{D\} = \left\{ \begin{array}{c} \vdots \\ (B_k - Y_{OLk})Y_{OLk}(1 - Y_{OLk}) \\ \vdots \end{array} \right\}_{n*1} \quad 17$$

Here B_j and B_k represent the target of the MFFN.

The $[S]$ matrix is estimated by

$$[S]_{m*n} = \{O\}_{\text{hidden } m*1} \langle D \rangle_{l*n} \quad 18$$

Then,

$$[\Delta W]_{m*n}^{t+1} = \alpha[\Delta W]_{m*n}^t + \eta[S]_{m*n} \quad 19$$

Here η and α represent the learning rate momentum coefficient of the network.

$$\{f\}_{m*l} = [W]_{m*n} \{D\}_{n*l} \quad 20$$

$$\{D^*\} = \left\{ \begin{array}{c} \vdots \\ f_i(Y_{HLi})(1 - Y_{HLi}) \\ \vdots \end{array} \right\}_{m*1} \quad 21$$

$$[Q]_{l*m} = \{Y\}_{IL \ l*1} \langle D^* \rangle_{l*m} = \{X\}_{IL \ l*1} \langle D^* \rangle_{l*m} \quad 22$$

Then,

$$[\Delta V]_{l*m}^{t+1} = \alpha[\Delta V]_{l*m}^t + \eta[Q]_{l*m} \quad 23$$

the new sets of weights for next training sets learning are computed by

$$[V]^{t+1} = [V]^t + [\Delta V]^{t+1} \quad 24$$

$$[W]^{t+1} = [W]^t + [\Delta W]^{t+1} \quad 25$$

Then,

$$\text{Error rate} = \frac{\sum \text{Error}_p}{n_{\text{set}}} \quad 26$$

Results and Discussion

In this article, a 10kW grid-connected solar PV power plant at the University of Technology and Applied Sciences, Ibb is considered for analysis. 4 solar PV array modules are used to generate electricity. Each array contains 5 solar PV modules with the specifications listed in Table 1.

Table 1. Specifications of solar PV panels

Specifications	Symbol	Values
Nominal power	P_{\max}	540W
Operating voltage	V_{mp}	41.3V
Operating current	I_{mp}	13.08 A
OC voltage	V_{oc}	49.2 V
SC current	I_{sc}	13.90A

The total production capacity of the solar PV system is 826V, 13.08A. The PV arrays are connected to a 1100V/230V grid-tied solar PV inverter, which has a rated output power of 10kW. A 10kW lighting load is connected to a solar PV inverter as a local load. The solar PV arrays are shown in Fig. 2. The solar PV inverter connected to the grid via DC and AC isolation switches is shown in Fig. 3.



Figure 2. Solar PV arrays



Figure 3. Solar PV inverter

Using the AI platform, the annual global solar irradiation level is estimated at the geographical

location of the plant site (23.24312 latitude and 56.4190 longitude) in UTAS, Ibri, as shown in Fig. 4

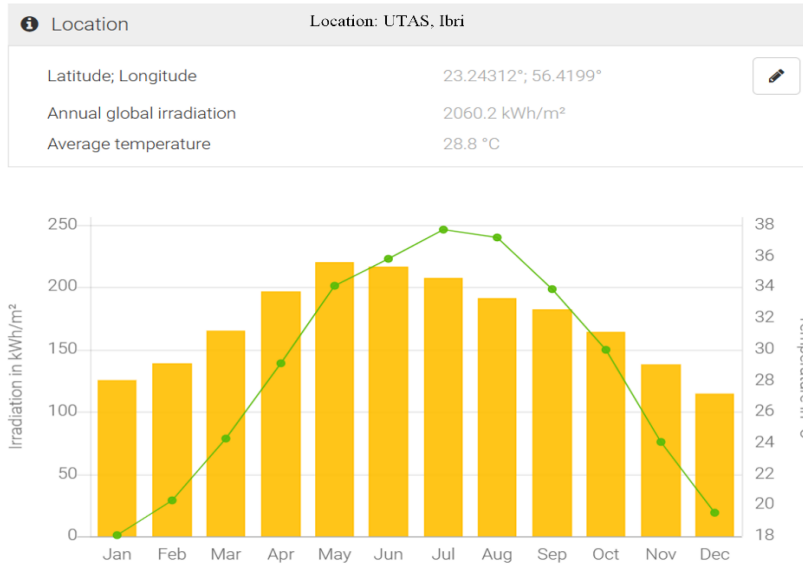


Figure 4. Annual global irradiation in UTAS, Ibri

It is observed that the annual global radiation amount in UTAS, Ibri, is 2060.2 kWh/m², with the average temperature measured at the site being 28.8 °C.

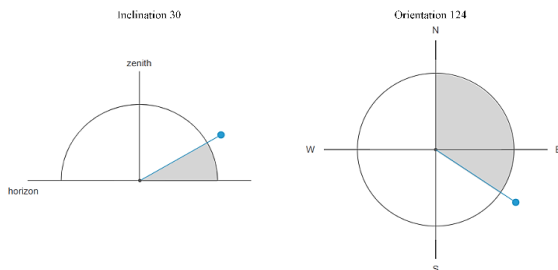


Figure 5. Inclination and orientation of the PV arrays

To achieve maximum performance with the MPPT controller, the solar PV systems are oriented at an angle of 124° in the southeast direction and tilted at an inclination of 30°, as shown in Fig. 5.



Figure 6. Annual power consumption of 10kW solar PV power plant

Fig. 6 shows the annual power consumption of a 10 kW solar PV power plant determined by the AI platform for the period January to December 2022 assuming a constant load. This is estimated using the climatic conditions during the period along with the annual global radiation level in UTAS, Ibri. Annual power consumption is estimated by AI to be 9360 kWh for the above period.

The MFFN is trained through training sets to monitor the performance of the solar PV system throughout the year in order to predict the solar PV power generation over the period of a year.

Training Set

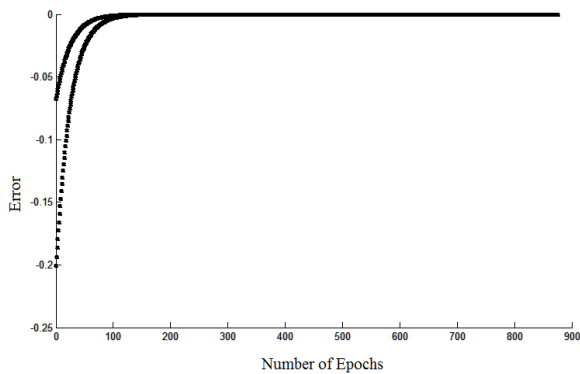
The output voltage and the power of the solar power system are considered as the training set for MFFN. The normalized input data sets collected from the solar PV system at different points in time are listed in Table 2. The first training set is trained by the MFFN is given in Table 3. The plot between error and number of epochs is shown in Fig. 7.

Table 2. The training data sets

Period (2022)	Normalized training data set
January 6, 8 AM	[0.19, 0.14]
March 15, 4 PM	[0.16, 0.28]
October 19, 1 PM	[0.31, 0.4]

Table 3. The error of the training set 1

Training set		Target		Input-Hidden layer weights	Hidden-output layer weights	Epochs	Error
V ₁	P ₁	V _t	P _t	[V11 V12 V21 V22]	[W11 W12 W21 W22]	n	Error _p
0.19	0.14	0.4279	0.5195	[0.2003 0.4000 0.1004 0.2000]	[0.2741 0.1910 0.5717 0.3901]	1	[-0.2010, -0.0675]
				[0.2046 0.4004 0.1049 0.2004]	[-0.2923 0.0015 -0.0461 0.1835]	50	[-0.0259 -0.0087]
				[0.2047 0.4004 0.1049 0.2004]	[-0.3651 -0.0228 -0.1254 0.1569]	100	[-0.0033 -0.0010]
				[0.2047 0.4004 0.1049 0.2004]	[-0.375 -0.0261 -0.1368 0.1534]	200	1.0e-004*
				[0.2047 0.4004 0.1049 0.2004]	[-0.3756 -0.0261 -0.1369 0.1534]	400	[-0.5397 -0.1457]
				[0.2047 0.4004 0.1049 0.2004]	[-0.3756 -0.0261 -0.1369 0.1534]	600	1.0e-007 *
				[0.2047 0.4004 0.1049 0.2004]	[-0.3756 -0.0261 -0.1369 0.1534]	876	[-0.1490 -0.0288]
				[0.2047 0.4004 0.1049 0.2004]	[-0.3756 -0.0261 -0.1369 0.1534]		1.0e-011 * [0 0]



The second training set is trained by the MFFN is given in Table 4. The plot between error and number of epochs is Fig. 8.

Figure 7. Plot between epochs and error for training set 1

Table 4. The error of the training set 2

Training set		Target		Input-Hidden layer weights	Hidden-output layer weights	Epochs	Error
V ₁	P ₁	V _t	P _t	[V11 V12 V21 V22]	[W11 W12 W21 W22]	n	Error _p
0.16	0.28	0.4321	0.5311	[0.2035 0.4004 0.1037 0.2005]	[-0.3586 0.0176 -0.1087 0.2037]	100	[-0.0038 -0.0010]
				[0.2035 0.4004 0.1037 0.2005]	[-0.3711 0.0142 -0.1222 0.2001]	200	1.0e-004 *
				[0.2035 0.4004 0.1037 0.2005]	[-0.3714 0.0142 -0.1225 0.2000]	400	[-0.7652 -0.1851]
				[0.2035 0.4004 0.1037 0.2005]	[-0.3714 0.0142 -0.1225 0.2000]	600	1.0e-007 *
				[0.2035 0.4004 0.1037 0.2005]	[-0.3714 0.0142 -0.1225 0.2000]	846	[-0.3087 -0.0588]
				[0.2035 0.4004 0.1037 0.2005]	[-0.3714 0.0142 -0.1225 0.2000]		1.0e-010 *
				[0.2035 0.4004 0.1037 0.2005]	[-0.3714 0.0142 -0.1225 0.2000]		1.0e-015 *
				[0.2035 0.4004 0.1037 0.2005]	[-0.3714 0.0142 -0.1225 0.2000]		[-0.1245 -0.0187] [-0.7772 0]

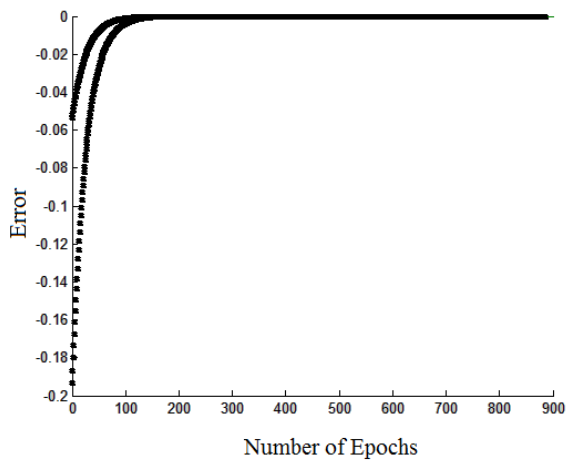


Figure 8. Plot between epochs and error for training set 2

The third training set is trained by the MFFN is given in Table 5. The plot between error and number of epochs is Fig. 9.

Table 5. The error of the training set 3

Training set		Target		Input-Hidden layer weights	Hidden-output layer weights	Epochs	Error
V _i	P _i	V _t	P _t	[V11 V12 V21 V22]	[W11 W12 W21 W22]	n	Error _p
0.31	0.4	0.4265	0.5159	[0.2043 0.4005 0.1045 0.2005]	[-0.3735 -0.0341 -0.1299 0.1463]	100	[-0.0036 -0.0012]
				[0.2043 0.4005 0.1045 0.2005]	[-0.3851 -0.0379 -0.1425 0.1422]	200	1.0e-004 *
				[0.2043 0.4005 0.1045 0.2005]	[-0.3854 -0.0379 -0.1428 0.1421]	400	1.0e-007 *
				[0.2043 0.4005 0.1045 0.2005]	[-0.3854 -0.0379 -0.1428 0.1421]	600	1.0e-011 *
				[0.2043 0.4005 0.1045 0.2005]	[-0.3854 -0.0379 -0.1428 0.1421]	835	1.0e-015 *
				[0.2043 0.4005 0.1045 0.2005]	[-0.3854 -0.0379 -0.1428 0.1421]		[-0.6106 0]

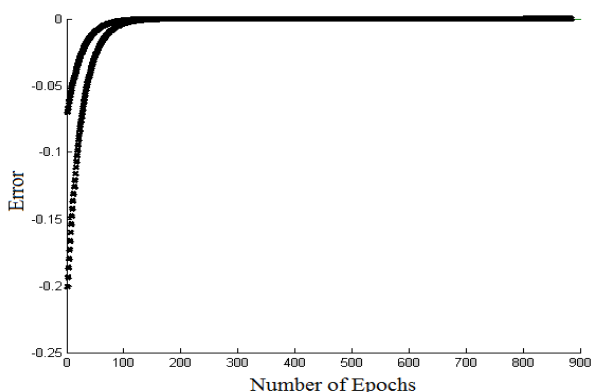


Figure 9. Plot between epochs and error for training set 3

each input data set individually. Based on Table 6, it can be inferred that the network required 76 epochs in order to reduce the discrepancy between the input and target data.

Test Set

Once the network is trained efficiently, it recognizes the input data set associated with the climatic conditions. Then the MFFN network is ready to predict the performance of the solar PV system for different climatic conditions in the UTAS, Ibri region. MFFN's updated input-hidden and hidden-output layer weights are given below for the test set

$$V_{t1} = \begin{bmatrix} 0.206 & 0.407 \\ 0.105 & 0.206 \end{bmatrix} W_{t1} = \begin{bmatrix} -0.424 & -0.047 \\ -0.232 & 0.153 \end{bmatrix}$$

Validation Set

In order to reduce the discrepancy between the input and target data, validation is carried out by running

Table 6. Validation set

Data set	Target	Epochs	Error
$[V_t, P_t]$	$[V_t, P_t]$	N	Error _p
[0.19, 0.14]	[0.16, 0.11]	1	[-0.210 -0.062]
[0.16, 0.4]	[0.18, 0.34]	2	[-0.178 -0.059]
[0.31, 0.2]	[0.35, 0.31]	3	[-0.189 -0.052]
.	.	.	[-0.151 -0.050]
.	.	.	[-0.106 -0.033]
.	.	.	[-0.072 -0.030]
.	.	.	[-0.049 -0.020]
.	.	.	[-0.031 -0.001]
.	.	.	[-0.022 -0.022]
.	.	.	[-0.026 -0.014]
.	.	.	[-0.0108 .004]
.	.	.	[-0.010 -0.004]
.	.	.	[-0.003 -0.002]
.	.	.	[-0.005 0.010]
.	.	.	[-0.003 -0.002]
.	.	.	[-0.005 -0.006]
.	.	.	[0.003 0.014]
.	.	.	[-0.005 -0.005]
.	.	.	[-0.007 -0.009]
.	.	.	[0.002 0.017]
[0.16, 0.4]	[0.18, 0.34]	76	1.0e-003 * [-0.306 0.5432]

Conclusion

The annual global irradiation and annual power consumption of the 10kW solar PV power system are predicted using an AI platform. The sample data set obtained from the solar PV system at different times of the year has shown that the data obtained by AI is accurate and very close to the real value. The results also show that the MFFN network is the most appropriate and suitable method for monitoring and predicting the performance of the solar PV system

for the different climatic conditions. The backpropagation algorithm used to train the MFFN network has also proven to be very effective for this application. In the future, the work can be extended to many other parameters of the solar PV system, such as: the solar radiation in the ground level, the ambient temperature and the surface temperature of the PV module. The work can also be extended with variable loads using the stochastic method.

Acknowledgment

The research was carried out in a 10 kW off-grid power plant at the University of Technology and Applied Sciences, Ibi, Sultanate of Oman.

Authors' Declaration

- Conflicts of Interest: None.
- We hereby confirm that all the Figures and Tables in the manuscript are ours. Furthermore, any Figures and images, that are not ours, have been included with the necessary permission for re-publication, which is attached to the manuscript.
- No animal studies are present in the manuscript.
- No human studies are present in the manuscript.
- Ethical Clearance: The project was approved by the local ethical committee at University of Technology and Applied Sciences, Oman.

Authors' Contribution Statement

G.K. and M.M.H.S. contributed to the research design, G.K., S.K., and Q.H.S.A.O conducted the analysis and writing of the manuscript.

References

1. Rahul I, Hariharan R. Enhancement of solar PV panel efficiency using double integral sliding mode MPPT control. *Tsinghua Sci Technol.* 2024; 29(1): 271-283. <https://doi.org/10.26599/TST.2023.9010030>.
2. Iyswarya AK, Rajaguru V, Vedanjali N, Pappula R. Solar forecasting for a PV battery powered DC system. *Heliyon.* 2023; 9(10). <https://doi.org/10.1016/j.heliyon.2023.e20667>.
3. Wang C, Li L. Efficient DC voltage balancing of cascaded photovoltaic system based on predictive modulation strategy. *IEEE Trans Ind Electron.* 2024; 71(2): 1514-1524. <https://doi.org/10.1109/TIE.2023.3253960>.
4. Al-Knani BA, Abdulkareem IH, Nemah HA, Nasir Z. Studying the changes in solar radiation and their influence on temperature trend in Iraq for a whole century. *Baghdad Sci J.* 2021; 18(2): 1076. [https://doi.org/10.21123/bsj.2021.18.2\(Suppl.\).1076](https://doi.org/10.21123/bsj.2021.18.2(Suppl.).1076).
5. Mahmood YH, Majeed MA. Design of a simple dust removal system for a solar street light system. *Baghdad Sci J.* 2022; 19(5): 1123. <https://doi.org/10.21123/bsj.2022.6467>.
6. Bakamba DDS, Souleymane S, Abdramane B. Data related to performance evaluation of an installed on-grid photovoltaic system at Bamako. *Data Brief.* 2023; 50. <https://doi.org/10.1016/j.dib.2023.109514>.
7. Gupta R, Ekata, Batra C. Performance assessment of solar-transformer-consumption system using neural network approach. *Baghdad Sci J.* 2022; 19(4): 0865. <https://doi.org/10.21123/bsj.2022.19.4.0865>.
8. Keaobaka K, Poti D, Raj MN, Nsilulu TMB, Ramesh CB. Intelligent solar photovoltaic power forecasting. *Energy Rep.* 2023; 9: 343-352. <https://doi.org/10.1016/j.egyr.2023.09.004>.
9. Dimd BD, Voller S, Midtgård OM, Cali U, Sevault A. Quantification of the impact of azimuth and tilt angle on the performance of a PV output power forecasting model for BIPVs. *IEEE J Photovolt.* 2024; 14(1): 194-200. <https://doi.org/10.1109/JPHOTOV.2023.3323809>.
10. Alshareef MJ. A comprehensive review of the soiling effects on PV module performance. *IEEE Access.* 2023; 11: 134623-134651. <https://doi.org/10.1109/ACCESS.2023.3337204>.
11. Martin JMA, Gyula G. Extensive comparison of physical models for photovoltaic power forecasting. *Appl Energy.* 2021; 283: 116239. <https://doi.org/10.1016/j.apenergy.2020.116239>.
12. Gonçalves A, Rativa D, Gómez MLA. Model-based assessment of the incident angle modifier on the annual angular losses and gain of PV modules in tracking systems. *IEEE J Photovolt.* 2023; 1-9. <https://doi.org/10.1109/JPHOTOV.2023.3323802>.
13. Mohamed E, Ashraf M, Mohamed MA, Francisco J, Salah K. Stochastic optimal power flow analysis of power systems with wind/PV/TCSC using a developed Runge Kutta optimizer. *J Electr Eng Technol.* 2023; 52. <https://doi.org/10.1016/j.ijepes.2023.109250>.
14. Shen X, Zheng Y, Zhang R. A hybrid forecasting model for the velocity of hybrid robotic fish based on back-propagation neural network with genetic algorithm optimization. *IEEE Access.* 2020; 8: 111731-111741. <https://doi.org/10.1109/ACCESS.2020.3002928>.
15. Zhang Y, Zheng W, Liu Z. Improving the spaceborne GNSS-R altimetric precision based on the novel multilayer feedforward neural network weighted joint prediction model. *Def Technol.* 2023; 1-4. <https://doi.org/10.1016/j.dt.2023.03.019>.
16. Mohammed NA, Al-Bazi A. An adaptive backpropagation algorithm for long-term electricity load forecasting. *Neural Comput Appl.* 2022; 34: 477-491. <https://doi.org/10.1007/s00521-021-06384-x>.

نموذج لمراقبة أداء الطاقة الشمسية الكهروضوئية والتنبؤ الإحصائي باستخدام الشبكة العصبية متعددة الطبقات والذكاء الاصطناعي

ج. كومار فيل¹، س. كيرثيجا²، محمد محمود حامد الشكلي¹، قيس حامد سيف عبد الله العثماني¹

¹قسم الهندسة، الجامعة التقنية والعلوم التطبيقية، عيري، عمان.

²القسم الكهربائي، شركة التصميم الفريد للصلب واللحام ذ.م.م، دبي، الامارات العربية المتحدة.

الخلاصة

إن الطبيعة الطبوغرافية لسلطنة عمان تجعل نظام الطاقة الشمسية خيارًا قابلاً للتطبيق وموثوقًا لإنتاج الطاقة بكميات كبيرة في سوق الطاقة المتجددة. تشهد العديد من المناطق الصحراوية في عمان مستويات عالية من الإشعاع الشمسي. وهذا مناسب للأنظمة الكهروضوئية لأن كفاءتها تعتمد بشكل أساسي على الإشعاع الشمسي. ومع ذلك، في التطبيقات في الوقت الفعلي، تؤثر العديد من العوامل البيئية على كفاءة الألواح الشمسية وبالتالي على أدائها. في هذه المقالة، تم اقتراح الشبكة الطبيعية (العصبية) الأمامية متعددة الطبقات (MFFN) لتتبع أداء نظام الطاقة الشمسية الكهروضوئية من أجل استبدال أو تحسين أداء نظام الطاقة الشمسية الكهروضوئية بناءً على حالته الحالية. يتم استخدام خوارزمية الانتشار العكسي (BPA) لتدريب MFFN.

الكلمات المفتاحية: خوارزمية الانتشار الخلفي، شبكة التغذية الأمامية متعددة الطبقات، النظام الكهروضوئي، الطاقة المتجددة، نظام الطاقة الشمسية.